

Hole mobility enhancement in $\text{In}_{0.41}\text{Ga}_{0.59}\text{Sb}$ quantum-well field-effect transistors

Ling Xia,^{1,a)} J. Brad Boos,² Brian R. Bennett,² Mario G. Ancona,² and Jesús A. del Alamo¹

¹*Microsystems Technology Laboratories, Massachusetts Institute of Technology (MIT), Cambridge, Massachusetts 02139, USA*

²*Naval Research Laboratory, Washington, DC 20375, USA*

(Received 3 January 2011; accepted 17 January 2011; published online 4 February 2011)

The impact of $\langle 110 \rangle$ uniaxial strain on the characteristics of p-channel $\text{In}_{0.41}\text{Ga}_{0.59}\text{Sb}$ quantum-well field-effect transistors (QW-FETs) is studied through chip-bending experiments. Uniaxial strain is found to affect the linear-regime drain current and the threshold voltage of the FET through the modulation of the hole mobility of the two-dimensional hole gas (2DHG) in the QW-FET. The piezoresistance coefficients of the 2DHG have been determined to be $\pi_{\langle 110 \rangle}^{\parallel} = 1.17 \times 10^{-10} \text{ cm}^2/\text{dyn}$ and $\pi_{\langle 110 \rangle}^{\perp} = -1.9 \times 10^{-11} \text{ cm}^2/\text{dyn}$. The value of $\pi_{\langle 110 \rangle}^{\parallel}$ is 1.5 times that of holes in Si metal-oxide-semiconductor (MOS) field-effect transistors and establishes InGaSb as a promising material system for a future III-V complementary MOS (CMOS) technology. © 2011 American Institute of Physics. [doi:10.1063/1.3552963]

In recent times, there has been great interest in exploring the substitution of the Si channel in scaled logic field-effect transistors (FETs) with a III-V compound semiconductor.¹ In this quest for a III-V complementary logic technology, realizing a high performance p-channel III-V FET remains a great challenge. One of the reasons lies in the enormous difference between the electron and hole transport properties in III-V's. The hole mobility in most III-V's is at best of the same order as in Si. A notable exception is InGaSb which exhibits a high Hall mobility of $\sim 1500 \text{ cm}^2/\text{V s}$ (Ref. 2) and has attracted considerable interest for future logic applications.³ Recently, p-channel InGaSb metal-oxide-semiconductor FETs (MOSFETs) with a high-quality dielectric interface have been demonstrated.⁴

A feasible approach to increase the hole mobility in the channel of a FET is to introduce strain. In fact, process-induced strain has become a crucial component of mainstream Si logic technology since the 90 nm node.⁵ Specifically, $\langle 110 \rangle$ uniaxial strain has been favored by industry because it brings a larger mobility enhancement along the strain direction than biaxial strain, especially under high surface electric field.⁶ In III-V systems, however, only a few reports^{4,7,8} exist that explore hole mobility enhancement through the introduction of $\langle 110 \rangle$ strain.

In this work, we carry out an experimental study of uniaxial strain effects on the hole mobility of two-dimensional hole gas (2DHG) in $\text{In}_{0.41}\text{Ga}_{0.59}\text{Sb}$ quantum-well field-effect transistors (QW-FETs), which is an excellent model system to study physics of relevance to future logic p-type MOSFET based on this material. Compared with a notable recent work on $\text{In}_{0.35}\text{Ga}_{0.65}\text{Sb}$ MOSFETs with Al_2O_3 gate dielectric,⁴ the structure studied in our work provides an epitaxy-quality heterostructure interface and the highest mobility in this material system to date.

Figure 1 shows the cross section of the InGaSb QW-FET used in this study. The fabrication process has been reported elsewhere.² This heterostructure is characterized by a Hall

mobility of $1500 \text{ cm}^2/\text{V s}$ and a sheet hole density (p_s) of $6.6 \times 10^{11} \text{ cm}^{-2}$. The channel is under 2.1% biaxial compressive strain, which contributes to the high hole mobility.⁹ The fabricated devices have a $0.2 \mu\text{m}$ gate length. Other electrical characteristics of these devices are given in Ref. 10.

$\langle 110 \rangle$ uniaxial strain was introduced to the QW-FET by a chip-bending apparatus.¹¹ Holes flow in the channel of these devices along the $[110]$ direction. A maximum of 0.08% strain parallel and perpendicular to the channel was sequentially applied to the same FET by rotating the chip by 90° . The stress is calculated using an estimated $\langle 110 \rangle$ Young's modulus (78 GPa) (Ref. 12) for the $\text{In}_{0.41}\text{Ga}_{0.59}\text{Sb}$. The strain at the chip surface is known within $\sim 3.5\%$. Changes in the device characteristics with strain were found to be recoverable. To minimize heating effects and parasitic Ohmic drops, the transfer characteristics at low V_{DS} (-50 mV) were measured. We focused on two figures of merit: the threshold voltage (V_{T} , extracted at $I_{\text{D}}=0.1 \text{ mA/mm}$) was initially used as a proxy to study device electrostatics, while the linear-regime drain current (I_{Dlin} , extracted at $V_{\text{GS}}-V_{\text{T}}=-0.2 \text{ V}$) was used to study the 2DHG channel mobility. The total channel resistance of our FET can be written as $R_{\text{ch}}=2R_{\text{c}}+2R_{\text{ext}}+R_{\text{int}}$, where R_{c} is the contact resistance between Ohmic metal and the 2DHG underneath it, R_{ext} is the resistance of the ungated semiconductor portion between the gate and the source/drain (S/D) contact metals, and R_{int} is the

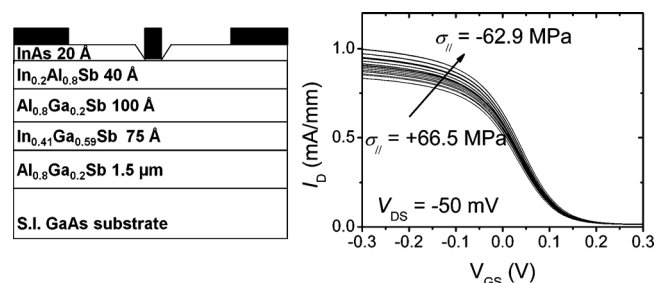


FIG. 1. (Left) The cross section of the $\text{In}_{0.41}\text{Ga}_{0.59}\text{Sb}$ QW-FET. (Right) Measured transfer characteristics as σ_{\parallel} changes.

^{a)}Electronic mail: lingxia@mit.edu.

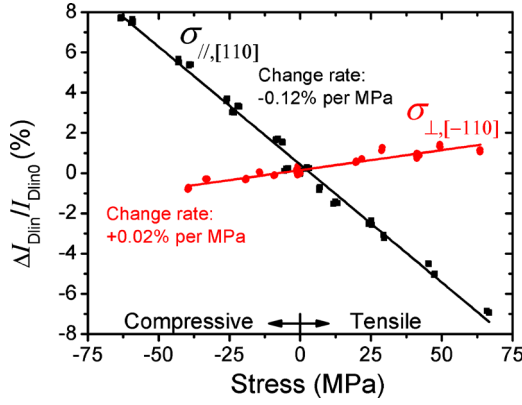


FIG. 2. (Color online) Relative change of linear-regime drain current at $V_{GS} - V_T = -0.2$ V as a function of $\langle 110 \rangle$ stress. Solid lines are linear fittings to the data.

resistance of the intrinsic region under gate. $2R_c$ measured by the transmission line method is $\sim 4 \Omega \text{ mm}$. This is $< 6\%$ of R_{tot} ($\sim 68 \Omega \text{ mm}$) at the bias of the I_{Dlin} extraction. R_{ext} is considered to be governed by similar strain effects as to R_{int} , except for a fixed 2DHG concentration of $6.6 \times 10^{11} \text{ cm}^{-2}$. Therefore, any impact from a fixed parasitic resistance arises only from $2R_c$, which can be safely neglected.

Figure 1 shows a representative example of the change in the transfer characteristics of an InGaSb QW-FET with stress applied along the channel direction ($\sigma_{||}$). A significant increase in I_{Dlin} with compressive stress ($\sigma < 0$) was observed.

Figure 2 summarizes the change of I_{Dlin} at $V_{GS} - V_T = -0.2$ V measured with both stress parallel ($\sigma_{||}$) and perpendicular (σ_{\perp}) to the channel. Significant anisotropic effects are seen: the magnitude of ΔI_{Dlin} under $\sigma_{||}$ is ~ 6 times higher than under σ_{\perp} ; the signs are also opposite for ΔI_{Dlin} with $\sigma_{||}$ and σ_{\perp} . For high gate overdrive, $-0.2 \text{ V} > V_{GS} - V_T > -0.4$ V (the maximum in this study), $\Delta I_{Dlin}/I_{Dlin}$ is found to be independent of V_{GS} . This is because at high gate overdrive, the intrinsic resistance (R_{int}) becomes small compared with that of the S/D regions (R_{ext}). Therefore, $\Delta I_{Dlin}/I_{Dlin}$ under high gate overdrive is dominated by $\Delta R_{ext}/R_{ext}$, and is independent of V_{GS} .

Attributing the change in I_{Dlin} to a change of μ_h requires some caution, because I_{Dlin} depends on p_s as well. Our previous study¹¹ showed that $\langle 110 \rangle$ uniaxial stress changes the two-dimensional (2D) carrier concentration in InGaAs QW-FETs through the piezoelectric effect by changing V_T and the gate capacitance (C_G). Shifts in V_T are also seen in the current devices (Fig. 3). However, changes of p_s due to the piezoelectric effect in the current InGaSb QW-FET are estimated to be negligible. One-dimensional Schrödinger-Poisson simulations show that Δp_s or ΔC_G due to the piezoelectric effect is 25 times smaller than the observed ΔI_{Dlin} . The reason is the tight confinement of 2DHG by the extremely thin quantum well (7.5 nm) and the small piezoelectric constants of the materials involved.¹³ Therefore, we can conclude that the observed ΔI_{Dlin} is induced by $\Delta \mu_h$. This requires a fresh explanation for the change in V_T seen in Fig. 3. We postulate that this is also caused by $\Delta \mu_h$.

Since we extract V_T at a constant current in the subthreshold regime, anything that affects the subthreshold current (I_{Dsub}) can propagate into an apparent change in V_T .

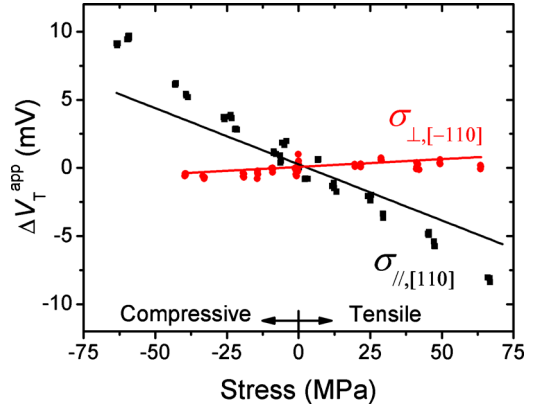


FIG. 3. (Color online) Change of measured or apparent threshold voltage as a function of $\langle 110 \rangle$ stress. The solid lines represent ΔV_T^{app} projected from $\Delta \mu_h$ according to Eq. (2).

Theoretically, carrier transport in the subthreshold regime of a FET follows a diffusion process.¹⁴ Therefore, I_{Dsub} depends on μ_h through the Einstein relation and the difference in p_s at the source and drain edges of the gate. Approximately, p_s depends linearly on the effective 2D density of states (DOS), and exponentially on V_{GS} .¹⁵ Therefore, for $V_{GS} - V_T \gg kT/q$,

$$I_{Dsub} \propto \mu_h \exp \frac{-q(V_{GS} - V_T)}{nkT}, \quad (1)$$

where n is the ideality factor, k is the Boltzmann constant, T is the temperature, and V_T is the threshold voltage which we define as the condition in which the Fermi level lines up with the top of the first subband in the channel.

This model suggests that I_{Dsub} is linearly proportional to μ_h . The proportionality constant in Eq. (1) contains the 2D DOS. $8 \times 8 \text{ k-p}$ simulations suggest that changes to the DOS due to strain are negligible [Fig. 4(c)] for our level of stress and only lead to $|\Delta V_T| < 0.5 \text{ mV}$. The parameters used in these simulations are according to Ref. 16. The effects of built-in biaxial strain and quantization are included in the

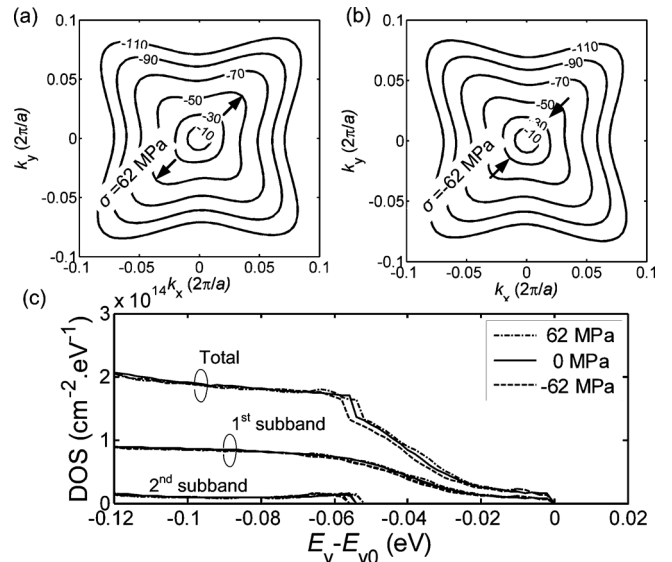


FIG. 4. In-plane dispersion relationship of the higher lying band in the $\text{In}_{0.41}\text{Ga}_{0.59}\text{Sb}$ QW under (a) 62 MPa tensile stress and (b) 62 MPa compressive stress. (c) Density of states in $\text{In}_{0.41}\text{Ga}_{0.59}\text{Sb}$ valence band for different values of stress. The change in density of states only leads to a marginal ΔV_T at the current level of stress.

simulations. In consequence, the change in apparent V_T measured at constant subthreshold current (ΔV_T^{app}) is indeed a shift of V_{GS} in the following way:

$$\Delta V_{GS} = \Delta V_T^{\text{app}} = \Delta V_T^{\text{elec}} + \frac{nkT}{q} \ln \left(1 + \frac{\Delta \mu_h}{\mu_h} \right). \quad (2)$$

ΔV_{GS} consists of a term that captures the change induced by device electrostatics (ΔV_T^{elec}) plus another term that includes mobility changes. ΔV_T^{elec} is affected by the piezoelectric effect and Schottky barrier height (ϕ_B) changes.¹¹ However, under the conditions of the present study, as mentioned above, the impact of the piezoelectric effect and Schottky barrier height changes on ΔV_T^{elec} are <0.5 and <0.6 mV, respectively. Therefore, we can conclude that ΔV_T^{app} is dominated by $\Delta \mu_h$ induced change.

As shown in Fig. 3, calculations of ΔV_T^{app} using this relation broadly agree with our experiments. The solid lines show the projected ΔV_T^{app} as a result of $\Delta \mu_h$ extracted from ΔI_{Dlin} . The projected ΔV_T^{app} matches relatively well with the apparent ΔV_T extracted from the subthreshold regime. The residual gap in Fig. 3 between the model and the data may be attributed to a larger $\Delta \mu_h / \Delta \sigma$ in the subthreshold regime than in the linear regime. This effect is akin to the decrease in the piezoresistance coefficients in p-type Si with increased carrier concentration.¹⁷

The piezoresistance coefficients ($\pi = -\Delta \mu / \mu \sigma$) of the $\text{In}_{0.41}\text{Ga}_{0.59}\text{Sb}$ 2DHG parallel and perpendicular to $\langle 110 \rangle$ uniaxial stress can then be calculated from the data in Fig. 2. They are found to be $\pi_{\langle 110 \rangle}^{\parallel} = 1.17 \times 10^{-10}$ cm²/dyn and $\pi_{\langle 110 \rangle}^{\perp} = -1.9 \times 10^{-11}$ cm²/dyn. Compared with $\pi_{\langle 110 \rangle}^{\parallel}$ for Si pMOS at a similar hole concentration (6.6×10^{11} cm⁻²),^{18,19} $\pi_{\langle 110 \rangle}^{\parallel}$ of the $\text{In}_{0.41}\text{Ga}_{0.59}\text{Sb}$ 2DHG is 1.5 times higher. This value is also 1.4 times higher than the $\pi_{\langle 110 \rangle}^{\parallel}$ found in an $\text{In}_{0.35}\text{Ga}_{0.65}\text{Sb}$ MOSFET in Ref. 4. Nevertheless, $\pi_{\langle 110 \rangle}^{\parallel}$ in Ref. 4 was probably measured at higher p_s ($>10^{12}$ cm⁻²), which might decrease its value.

The anisotropic behavior of the piezoresistance coefficients of $\text{In}_{0.41}\text{Ga}_{0.59}\text{Sb}$ qualitatively agrees with the trend seen in Si. This is partly due to the anisotropic response of the valence band to $\langle 110 \rangle$ uniaxial strain as seen in our $k \cdot p$ simulations (Fig. 4). More sophisticated calculations²⁰ are needed to theoretically quantify the change in hole mobility. A final remark is that the piezoresistance coefficients are measured for $\text{In}_{0.41}\text{Ga}_{0.59}\text{Sb}$ channel with 2.1% compressive biaxial strain and quantum confinement. These coefficients could be different under other built-in biaxial strain or confinement conditions.

In summary, we have experimentally studied the impact of $\langle 110 \rangle$ uniaxial strain on the electrical characteristics on p-channel $\text{In}_{0.41}\text{Ga}_{0.59}\text{Sb}$ QW-FETs. We have found that $\langle 110 \rangle$ uniaxial strain can significantly enhance the hole mobility in these devices. The conclusion is confirmed by analysis consisting of Schrödinger–Poisson simulations, $k \cdot p$ simu-

lations, and our model which reveals the relation between observed change in drain current and threshold voltage. The piezoresistance coefficients are determined to be $\pi_{\langle 110 \rangle}^{\parallel} = 1.17 \times 10^{-10}$ cm²/dyn and $\pi_{\langle 110 \rangle}^{\perp} = -1.9 \times 10^{-11}$ cm²/dyn. $\pi_{\langle 110 \rangle}^{\parallel}$ is 1.5 times more than in Si. Therefore, process-induced uniaxial strain should be valuable for enhancing the performance of p-channel $\text{In}_{0.41}\text{Ga}_{0.51}\text{Sb}$ QW-FETs. When coupled with its high hole mobility, $\text{In}_{0.41}\text{Ga}_{0.51}\text{Sb}$ emerges as a promising channel material for future high performance p-type logic FETs.

The MIT portion of this work was sponsored by FCRP-MSD and Intel Corp. The NRL authors thank the Office of Naval Research for support.

- ¹D.-H. Kim and J. A. del Alamo, Tech. Dig. - Int. Electron Devices Meet. **2009**, 861.
- ²J. B. Boos, B. R. Bennett, N. A. Papanicolaou, M. G. Ancona, J. G. Champlain, R. Bass, and B. V. Shanabrook, *Electron. Lett.* **43**, 834 (2007).
- ³M. Radosavljevic, T. Ashley, A. Andreev, S. D. Coomber, G. Dewey, M. T. Emeny, M. Fearn, D. G. Hayes, K. P. Hilton, M. K. Hudait, R. Jefferies, T. Martin, R. Pillarisetty, W. Rachmady, T. Rakshit, S. J. Smith, M. J. Uren, D. J. Wallis, P. J. Wilding, and R. Chau, Tech. Dig. - Int. Electron Devices Meet. **2008**, 727.
- ⁴A. Nainani, T. Irisawa, Z. Yuan, Y. Sun, T. Krishnamohan, M. Reason, B. R. Bennett, J. B. Boos, M. G. Ancona, Y. Nishi, and K. C. Saraswat, Tech. Dig. - Int. Electron Devices Meet. **2010**, 138.
- ⁵K. Mistry, M. Armstrong, C. Auth, S. Cea, T. Coan, T. Ghani, T. Hoffmann, A. Murthy, J. Sandford, R. Shaheed, K. Zawadzki, K. Zhang, S. Thompson, and M. Bohr, Tech. Dig. VLSI Symp. **2004**, 50.
- ⁶S. Thompson, G. Sun, K. Wu, J. Lim, and T. Nishida, Tech. Dig. - Int. Electron Devices Meet. **2004**, 221.
- ⁷A. Nainani, J. Yum, J. Barnett, R. Hill, N. Goel, J. Huang, P. Majhi, R. Jammy, and K. C. Saraswat, *Appl. Phys. Lett.* **96**, 242110 (2010).
- ⁸A. Nainani, D. Kim, T. Krishnamohan, and K. Saraswat, Proceedings of the International Conference on Simulation of Semiconductor Processes and Devices, 2009, p. 47.
- ⁹B. R. Bennett, M. G. Ancona, J. B. Boos, and B. V. Shanabrook, *Appl. Phys. Lett.* **91**, 042104 (2007).
- ¹⁰J. B. Boos, B. R. Bennett, N. A. Papanicolaou, M. G. Ancona, J. G. Champlain, Y.-C. Chou, M. D. Lange, J. M. Yang, R. Bass, D. Park, and B. V. Shanabrook, *IEICE Trans. Electron.* **E91-C**, 1050 (2008).
- ¹¹L. Xia and J. A. del Alamo, *Appl. Phys. Lett.* **95**, 243504 (2009); **97**, 029901(E) (2010).
- ¹²S. Adachi, *Handbook on Physical Properties of Semiconductors* (Springer, Berlin, 2004), pp. 453 & 625.
- ¹³G. Arlt and P. Quadflieg, *Phys. Status Solidi B* **25**, 323 (1968).
- ¹⁴S. M. Sze, *The Physics of Semiconductor Devices* (Wiley, New York, 1981).
- ¹⁵S. Karmalkar, *IEEE Trans. Electron Devices* **44**, 862 (1997).
- ¹⁶I. Vurgaftman, J. R. Meyer, and L. R. Ram-Mohan, *J. Appl. Phys.* **89**, 5815 (2001).
- ¹⁷Y. Kanda, *IEEE Trans. Electron Devices* **29**, 64 (1982).
- ¹⁸S. E. Thompson, S. Suthram, Y. Sun, G. Sun, S. Parthasarathy, M. Chu, and T. Nishida, Tech. Dig. - Int. Electron Devices Meet. **2006**, 1.
- ¹⁹K. Uchida, R. Zednik, L. Ching-Huang, H. Jagannathan, J. McVittie, P. C. McIntyre, and Y. Nishi, Tech. Dig. - Int. Electron Devices Meet. **2004**, 229.
- ²⁰M. V. Fischetti, Z. Ren, P. M. Solomon, M. Yang, and K. Rim, *J. Appl. Phys.* **94**, 1079 (2003).